

Energy Transfer in Isotropic Turbulence

MAHINDER S. UBEROI

*Department of Aerospace Engineering Sciences and Joint Institute for Laboratory Astrophysics,
University of Colorado, Boulder, Colorado*

and

*Department of Aeronautical and Astronautical Engineering, The University of Michigan,
Ann Arbor, Michigan*

(Received 19 October 1962; revised manuscript received 3 May 1963)

Energy transfer from large to small eddies at three stations in turbulence behind a square mesh is determined by measuring the rates of change and viscous dissipation of the spectrum and the results are compared with a theoretical prediction. Large eddies for which viscous dissipation is negligible satisfy a similarity relation which agrees with the fact that the total energy decays as some negative power of time. Small eddies which are in approximate statistical equilibrium satisfy local similarity according to Kolmogoroff. Various terms in the vorticity equation are also determined and the quantities representative of small scale motion are universal constants when expressed in terms of Kolmogoroff parameters.

INTRODUCTION

LET us consider a large volume of an incompressible fluid which is homogeneously stirred and then left to decay. Define an energy spectrum E such that $E dk$ is the average amount of kinetic energy per unit mass of fluid with wavenumber between k ($= 2\pi/\text{wavelength}$) and $k + dk$. The total energy

$$\frac{1}{2}(\overline{u^2} + \overline{v^2} + \overline{w^2}) = \int_0^\infty E(k, t) dk, \quad (1)$$

where an overbar denotes an average. The spectrum will show a maximum at a wavenumber which is approximately inversely proportional to the length characterizing the stirrer. The equation governing E is obtained by suitably averaging the equation of motion¹

$$(\partial/\partial t)E(k, t) = \underset{\text{rate of transfer}}{T(k, t)} - \underset{\text{rate of viscous dissipation}}{2\gamma k^2 E(k, t)}. \quad (2)$$

We have one equation and two unknowns. This indetermination is due to the averaging process. It is necessary to postulate a relation between the rate of transfer T and the spectrum E before we can solve for $E(k, t)$ in terms of $E(k, 0)$.

The validity of the postulate may be checked by comparing the measured with the predicted spectrum. However, the measurement of energy transfer is a more direct check on the validity of the theory and brings out the essential features of the problem. In many statistical problems it is not possible to directly check the hypothesis used to complement the averaged equations, only its consequences are subject to experimental observation. For instance,

in the kinetic theory of dense gas it is necessary to assume a relation between the probability of collision involving $(n + 1)$ particles with that involving n particles. It is rather difficult to check this assumption, only the consequences are subject to examination. In this respect we are somewhat fortunate. The energy transfer has been determined by measuring the rate of change of E and adding to it the rate of viscous loss. The results are discussed in view of the current ideas on turbulence.

EXPERIMENTAL ARRANGEMENT AND TECHNIQUES

All measurements were made in 2×2 -ft low turbulence wind tunnel behind one inch square mesh biplane grid made of $\frac{1}{4}$ -in. round wooden dowels at a mean speed $U_0 = 51.5$ ft/sec. The grid Reynolds number $U_0 M/\nu$ was 2.64×10^4 where M is the grid mesh length. Without the grid $\overline{u^2}/U_0^2 = 2 \times 10^{-8}$ and $\overline{v^2}/U_0^2 = 9 \times 10^{-8}$ which are much smaller than those produced by the grid to be of any consequence. Measurements of fluctuating velocities were made with a compensated constant current platinum hot-wire anemometer which responds faithfully from 2 to 2×10^4 cps. The wire had a diameter of 10^{-4} in. and length of 16×10^{-3} in. A straight wire was used to measure u and an x wire to measure v .

Measurements of $(u + \sqrt{2} v)$ were made by placing a single wire in the (x, y) plane inclined to the mean flow which is in x direction. It is sensitive to both u and v . Although various relations for the hot-wire sensitivity to u and v have been suggested they are notoriously inadequate for making precise measurements. The response of the wire to u was determined by sinusoidally oscillating the wire in the x direction at 3 cps and at various amplitudes. The

¹ W. Heisenberg, *Z. Phys.* **124**, 628 (1948).

response to v was determined by sinusoidally rotating the wire about the z axis. The angle of rotation for small values is equal to v/U . The inclination of the wire to the mean motion is adjusted such that its sensitivity to v is $\sqrt{2}$ times its sensitivity to u and the output of the wire is therefore proportional to $u + \sqrt{2} v$.

This calibration procedure has another advantage. Normally we calibrate the hot wire at constant resistance and use it at constant current under the assumption that the wire resistance is proportional to its temperature. This assumption can introduce considerable error if the wire temperature is high.

DECAY OF TOTAL ENERGY

The inverse of the measurements of \bar{u}^2/U_0^2 , \bar{v}^2/U_0^2 , and $(\bar{u}^2 + 2\bar{v}^2)/3U_0^2$ as a function of distance behind the grid or x/M , where M is the grid mesh, length, are shown in Fig. 1. The ratio \bar{u}^2/\bar{v}^2 is also shown there and has a nearly constant value of 1.45 indicating that grid generated turbulence is not strictly isotropic and there is no strong tendency for it to become so further downstream. The quantity

$$\frac{U_0^2}{\bar{u}^2 + 2\bar{v}^2} \bigg/ \frac{d}{dx} \left(\frac{U_0^2}{\bar{u}^2 + 2\bar{v}^2} \right)$$

as a function of x is shown in Fig. 2 and varies approximately linear with x and has a slope of 1/1.2. It follows that

$$\begin{aligned} \bar{u}^2 + 2\bar{v}^2 &\sim (x - x_0)^{-1.2} \\ &\sim (t - t_0)^{-1.2}; \quad t = x/U_0, \end{aligned} \quad (3)$$

where x_0 is a constant.

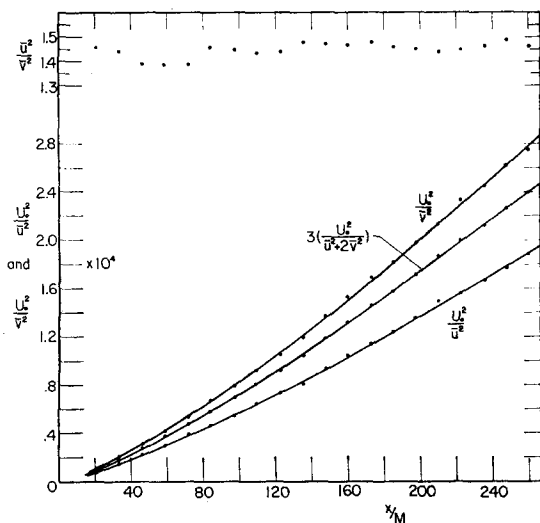


FIG. 1. Decay of turbulence behind the grid and the ratio \bar{u}^2/\bar{v}^2 .

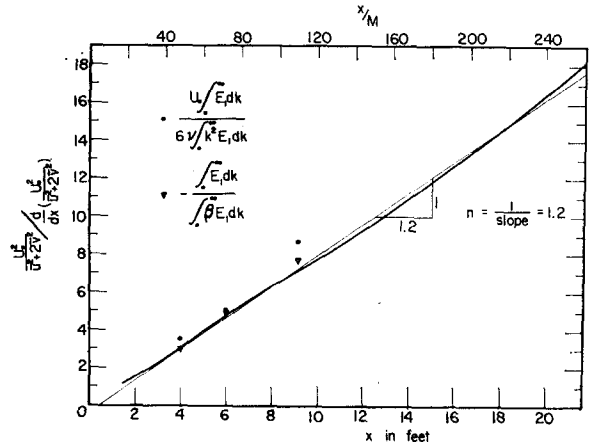


FIG. 2. The function $[U_0^2/(\bar{u}^2 + 2\bar{v}^2)] [(dU_0^2/dt)/(\bar{u}^2 + 2\bar{v}^2)]^{-1}$ as determined from the decay of turbulence.

SPECTRUM OF TURBULENCE

The three-dimensional spectrum E which appears in Eq. (2) cannot be measured directly. However, it is possible to measure a one-dimensional spectrum E_1 . In the case of isotropic turbulence, the two are related by the equation

$$E(k, t) = -\frac{1}{2}k(\partial/\partial k)E_1(k, t). \quad (4)$$

The one-dimensional spectrum of \bar{u}^2 and \bar{v}^2 are different but those of \bar{v}^2 and \bar{w}^2 are identical when u, v , and w are given as functions of x . The function E_1 is the spectrum¹ of $\bar{u}^2 + 2\bar{v}^2$, i.e.,

$$\bar{u}^2 + 2\bar{v}^2 = \int_0^\infty E_1(k, t) dk. \quad (5)$$

It gives the sum of the diagonal elements of the spectral tensor and has the advantage that E can be determined from E_1 by a single differentiation. If we had measured the spectrum of either \bar{u}^2 or \bar{v}^2 then it would have been necessary to differentiate the measured spectrum twice in order to get E . Furthermore, by measuring the spectrum of the total energy $\bar{u}^2 + 2\bar{v}^2$, we minimize the effect of anisotropy of grid generated turbulence when E is determined from E_1 since Eq. (4) is valid for isotropic turbulence only.

In actual practice a straight hot-wire is placed at a fixed distance behind the grid. The inclination of the wire to mean motion is adjusted such that its output is proportional to $(u + \sqrt{2} v)$. If we assume that turbulence is essentially convected downstream ($t = x/U_0$) then $u(t) + \sqrt{2} v(t) = u(x/U_0) + \sqrt{2} v(x/U_0)$, i.e., the measurement of velocity fluctuations at one point gives the spatial velocity fluctuations as a function of x . The output

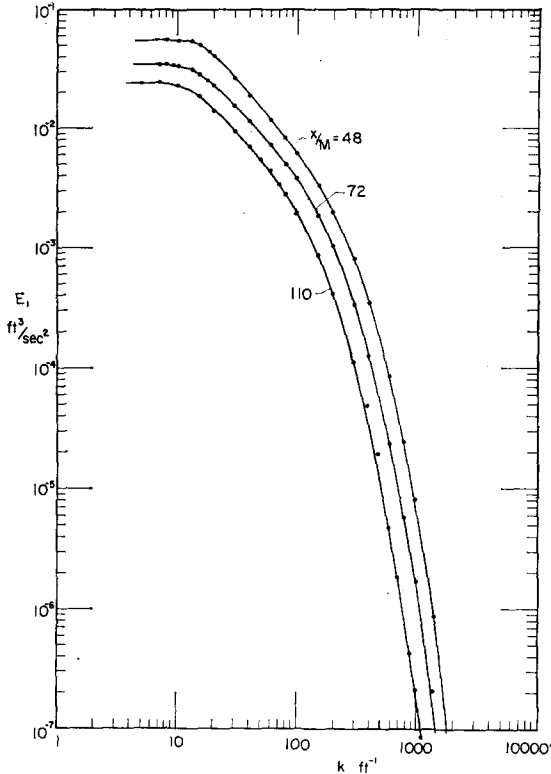


FIG. 3. The spectra E_1 at the three stations behind the grid.

of the hot wire is passed through a selective filter of narrow pass band with variable center frequency of 0 to 16 kc/sec. The mean-square output of the selective filter was measured with a thermocouple and an integrator. The result gives E_1 as a function of frequency or wavenumber $k (= 2\pi U_0/\text{frequency})$. The measured spectra at $x/M = 48, 72,$ and 110 are shown in Fig. 3.

The spectrum E was determined by measuring the slopes of the above curves as functions of k ,

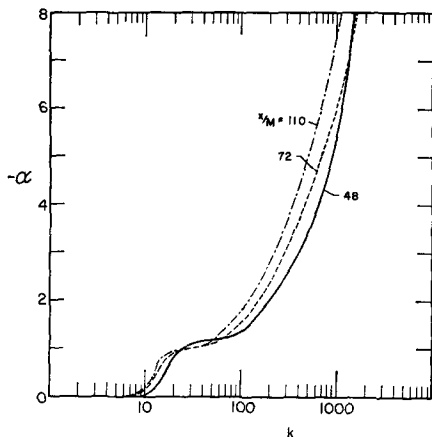


FIG. 4. Logarithmic slope of E_1 .

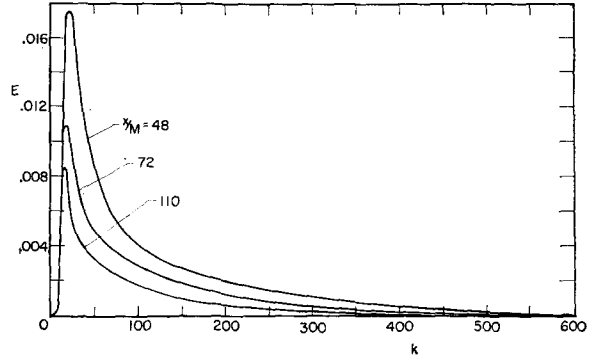


FIG. 5. The spectra E at the three stations.

$$\alpha(k, t) = \frac{\partial \ln E_1}{\partial \ln k} = \frac{k}{E_1} \frac{\partial E_1}{\partial k} \quad (6)$$

so that

$$E = -\frac{k}{2} \frac{\partial}{\partial k} E_1 = -\frac{1}{2} \alpha E_1. \quad (7)$$

This method of determining E from E_1 is more accurate than the direct differentiation since E_1 varies by a factor of 10^5 . The function α can be determined quite accurately and is a smoothly varying function of k as shown in Fig. 4. The computed E 's are shown in Fig. 5 and show a maxima at $k \sim 1/M$. The value of E for $k > 600$ is too small to show in the figure and may be determined by using Eq. (7) and the data in Figs. 3 and 4. Due to finite length of the hot wire, E_1 was corrected according to the method given in reference 2. However, this correction was never more than 8% of the measured E_1 .

RATE OF CHANGE OF SPECTRUM

The rate of change of E is determined from that of E_1 by using the relation

$$\frac{\partial E}{\partial t} = -\frac{k}{2} \frac{\partial}{\partial k} \left(\frac{\partial E_1}{\partial t} \right). \quad (8)$$

The spectrum E_1 was measured as a function of x for a fixed k and the slope

$$\beta(k, t) = \frac{\partial \ln E_1}{\partial x} = \frac{1}{U_0 E_1} \frac{\partial E_1}{\partial t} \quad (9)$$

was measured. The process was repeated to get β as a function of k . The measured β for $x/M = 48, 72,$ and 110 are shown in Fig. 6 and show that the rate of change of E_1 increases with k . The slopes

$$\gamma(k, t) = \partial \ln \beta E_1 / \partial \ln k \quad (10)$$

² M. S. Uberoi and L. S. G. Kovaszny, Princeton University, Project Squid, Rept. No. 30, (1952).

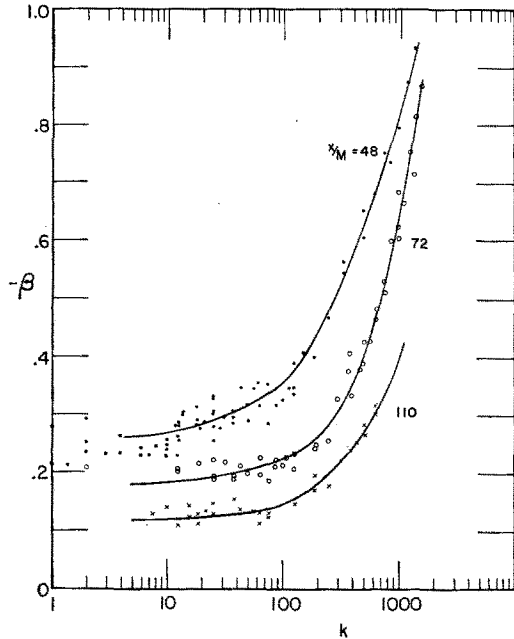


FIG. 6. Relative decay $(1/U_0 E_1)(\partial/\partial t) E_1$, of the spectral components.

were measured for $x/M = 48, 72,$ and 110 as functions of k and are shown in Fig. 7.

It follows from Eqs. (4) and (10) that

$$\partial E/\partial t = -\frac{1}{2}U_0\gamma(k, t)\beta(k, t)E_1. \quad (11)$$

The function $\partial E/\partial t$ thus determined for the three stations is shown in Fig. 8 and show that its value is insignificant for large k . The self-consistency of measurement requires that

$$\int_0^\infty \frac{\partial E}{\partial t} dk = -\frac{U_0}{2} \int_0^\infty \gamma\beta E_1 dk$$

or

$$\frac{d}{dt} (\overline{u^3} + 2\overline{v^2}) = -U_0 \int_0^\infty \gamma\beta E_1 dk. \quad (12)$$

The measured values for the two sides of this equation are shown in Fig. 2 showing agreement within a few percent.

ENERGY TRANSFER

The viscous dissipation of energy per unit wave-number

$$-2\nu k^2 E = -k^2 \alpha E_1 \quad (13)$$

can be determined from the available data and the results are shown in Fig. 9. The energy transfer is given by the relation

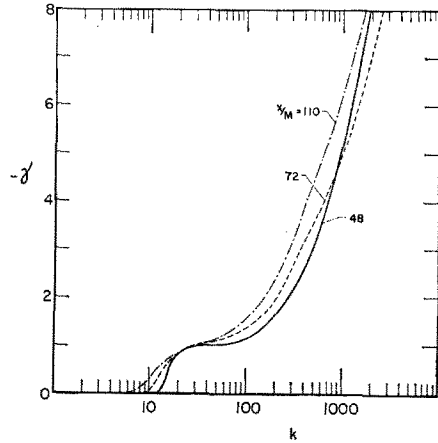


FIG. 7. The function $\gamma = \partial \ln \beta E/\partial \ln k$.

$$T(k, t) = (\partial/\partial t)E(k, t) + 2\nu k^2 E(k, t). \quad (14)$$

Since the total transfer is zero

$$\int_0^\infty \frac{\partial E}{\partial t} dk = -2\nu \int_0^\infty Ek^2 dk$$

or

$$\frac{U_0}{2} \int_0^\infty \gamma\beta E_1 dk = 2\nu \int_0^\infty Ek^2 dk. \quad (15)$$

The measured values for the two sides of the equation are shown in Fig. 2. The right hand side is smaller than the left hand by 13%, 4%, and 13% at $x/M = 48, 72,$ and $110,$ respectively. This may be due to anisotropy of the grid generated turbulence since Eq. (14) is valid for isotropic turbulence only. At each station β was multiplied by a constant factor so that Eq. (15) is satisfied. The plots of

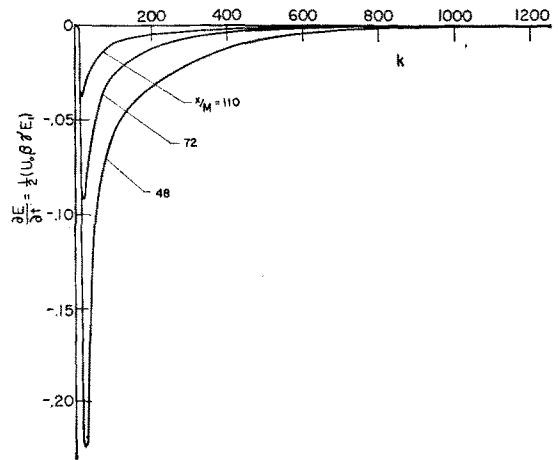


FIG. 8. The function $\partial E/\partial t$.

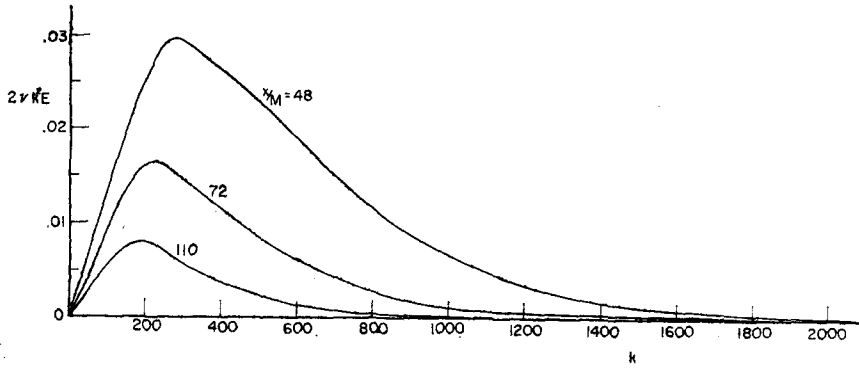


FIG. 9. Viscous dissipation of the spectra.

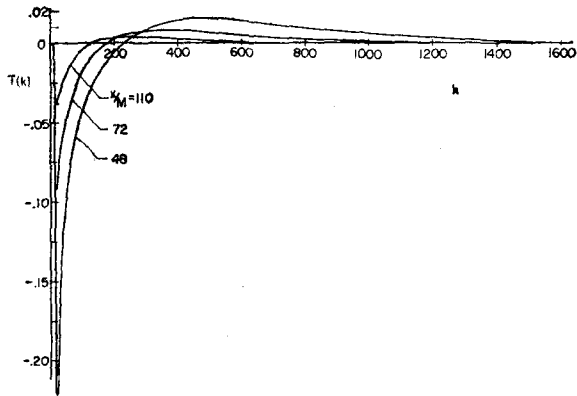


FIG. 10. Energy transfer at the three stations.

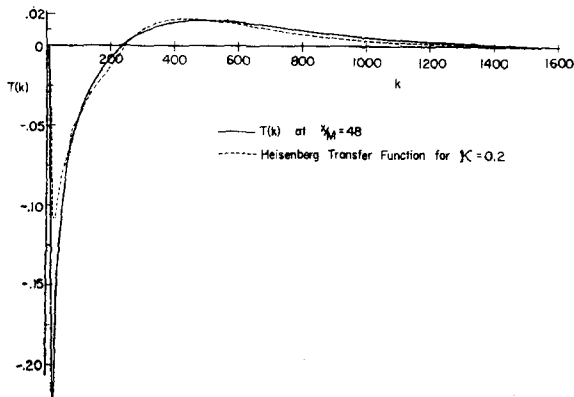


FIG. 11. Comparison of measured transfer with Heisenberg's prediction for $x/M = 48$.

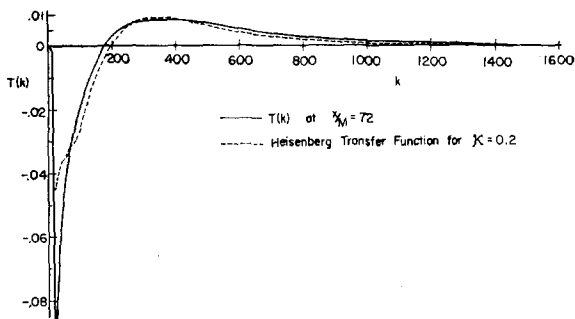


FIG. 12. Comparison of measured transfer with Heisenberg's prediction for $x/M = 72$.

$\partial E/\partial t$ in Fig. 8 are based on β thus adjusted. The energy transfer determined from Eq. (14) using measured rates of change of spectrum and viscous decay are shown in Fig. 10.

THEORETICAL PREDICTIONS ABOUT ENERGY TRANSFER

Various investigators have proposed hypotheses relating T with E , none of which is accurate. Here we compare the experimental results with Heisenberg's theory which states that

$$T = 2\mathcal{K} \left\{ -Ek^2 \int_k^\infty \left[\frac{E(x, t)}{k^3} \right]^{\frac{1}{2}} dx - \left(\frac{E}{k^3} \right)^{\frac{1}{2}} \int_0^k Ey^2 dy \right\} \tag{16}$$

where \mathcal{K} is a universal constant. The measured E was used to calculate T according to the above equation and the results are compared with the measurements in Figs. 11, 12, and 13. The universal constant \mathcal{K} can take a wide range of values depending on the region of k over which the prediction is made to fit the observations. This is a major drawback of the theory.

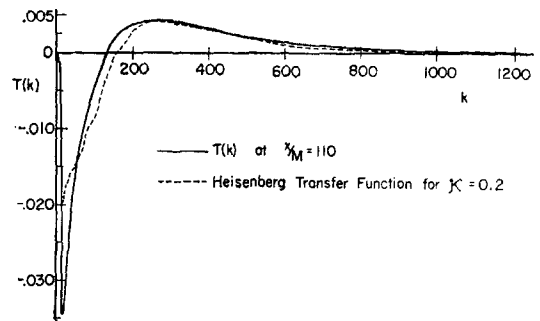


FIG. 13. Comparison of measured transfer with Heisenberg's prediction for $x/M = 110$.

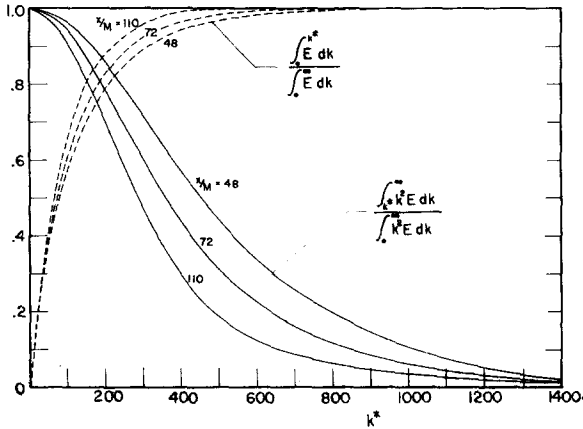


FIG. 14. Energy containing and energy dissipating eddies.

SIMILARITY OF LARGE EDDIES

The ratios

$$\int_0^{k^*} E dk / \int_0^\infty E dk \quad \text{and} \quad \int_{k^*}^\infty Ek^2 dk / \int_0^\infty Ek^2 dk$$

as functions of k^* are given in Fig. 14 and show that it is possible to approximately divide the entire motion into energy containing eddies with wavenumbers from 0 to k^* and dissipating eddies with wavenumbers from k^* to ∞ . The ratio of the rates of change to the viscous dissipation of spectrum is given in Fig. 15 and show that small eddies are approximately in statistical equilibrium and for large eddies

$$\partial E(k, t) / \partial t \doteq T(k, t). \tag{17}$$

This relation was first postulated by Kármán and Howarth³ for high Reynolds number. The present interpretation is that it is valid for energy con-

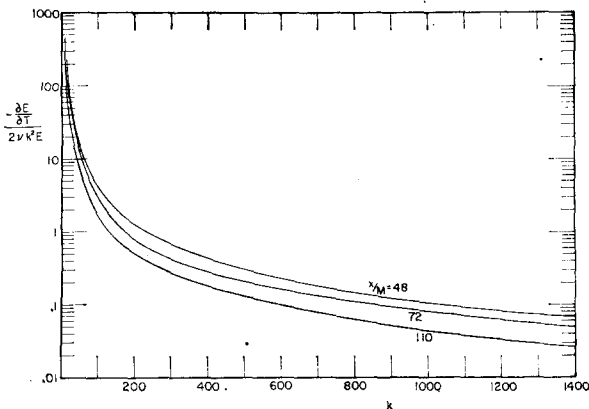


FIG. 15. The ratio $-(\partial E / \partial t) / 2\nu k^2 E$.

³ T. Kármán and L. Howarth, Proc. Roy. Soc. (London) A164, 192 (1938).

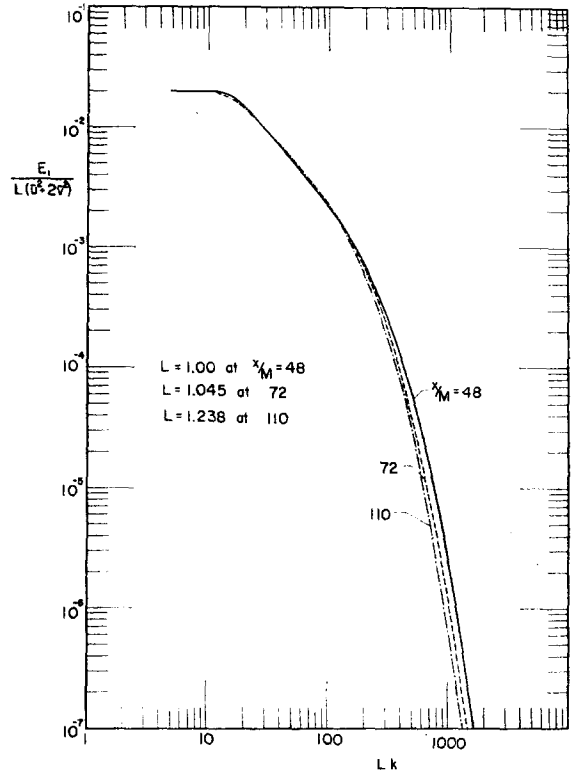


FIG. 16. Similarity of E_1 for large eddies.

taining eddies for practically all Reynolds numbers.

The energy containing eddies show a similarity such that

$$E_1(k, t) = (\overline{u^2} + 2\overline{v^2})L(t)F_1(kL), \tag{18}$$

$$E(k, t) = \frac{1}{2}(\overline{u^2} + 2\overline{v^2})L(t)F(kL), \tag{19}$$

$$T(k, t) = (\overline{u^2} + 2\overline{v^2})^{\frac{3}{2}} \Gamma(kL), \tag{20}$$

where $L(t)$ is a length characteristic of these eddies and F_1, F , and Γ are functions of one variable kL . Figures 16, 17, and 18 confirm this similarity for k in the range of energy containing eddies. Equation (17), which is valid for this range of k , becomes

$$F(kL) \frac{d}{dt} \left(\frac{\overline{u^2} + 2\overline{v^2}}{2} \right) L + \left(\frac{\overline{u^2} + 2\overline{v^2}}{2} \right) (F'kL) \frac{d}{dt} \left(\frac{\overline{u^2} + 2\overline{v^2}}{2} \right) = \left(\frac{\overline{u^2} + 2\overline{v^2}}{2} \right)^{\frac{3}{2}} \Gamma(kL). \tag{21}$$

In order that this be a total differential equation, we must have that

$$\left(\frac{\overline{u^2} + 2\overline{v^2}}{2} \right)^{-\frac{1}{2}} \frac{dL}{dt}$$

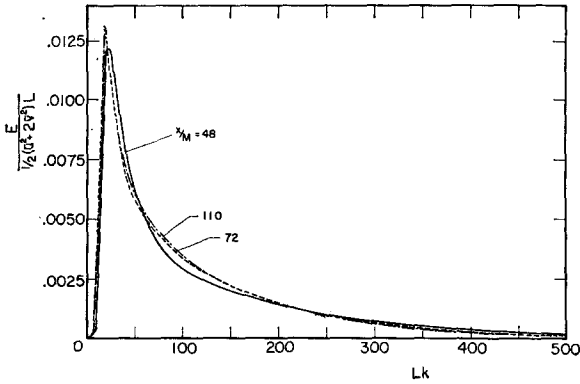


FIG. 17. Similarity of E for large eddies.

and

$$\left(\frac{\bar{u}^2 + 2\bar{v}^2}{2}\right)^{-\frac{1}{2}} \frac{d}{dt} \left[\frac{1}{2}L(\bar{u}^2 + 2\bar{v}^2)\right]$$

are constants, or

$$(\bar{u}^2 + 2\bar{v}^2) \sim (t - t_0)^{-n} \tag{22}$$

and

$$L \sim (t - t_0)^{1-\frac{1}{2}n} \tag{23}$$

The measurements of energy decay in Fig. 2 show that approximately $n = 1.2$ and therefore

$$L \sim (t - t_0)^{0.4} \tag{24}$$

Neglecting t_0 which is small, the variation of L with t or $x (=U_0t)$ is shown in Fig. 19.

We have found that the value of n varies somewhat with the type of grid. This work will be reported elsewhere.

UNIVERSAL EQUILIBRIUM OF SMALL EDDIES

Figures 14 and 15 show that small eddies responsible for viscous dissipation are in approximate statistical equilibrium and according to Kolmo-

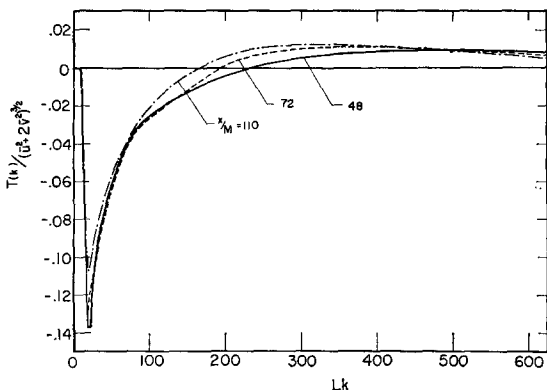


FIG. 18. Similarity of T for large eddies.

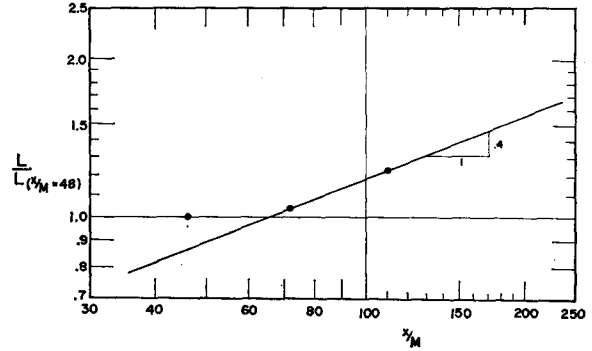


FIG. 19. Variation of the length L characteristic of large eddies

goroff's⁴ first similarity hypothesis lk^2E/v_K is a universal function of lk , where

$$v_K = (\nu\varepsilon)^{\frac{1}{2}}, \quad l = \left(\frac{\nu^3}{\varepsilon}\right)^{\frac{1}{2}}$$

$$\text{and } \varepsilon = -\frac{d}{dt}(\bar{u}^2 + 2\bar{v}^2) = 2 \int_0^\infty Ek^2 dk.$$

The measured spectra at the three stations are plotted in Fig. 20 in terms of the above parameters and show agreement with the theory. Other investigators have measured one-dimensional spectrum of \bar{u}^2 and plotted it for small eddies in terms of the above parameters. We could compute the spectrum of \bar{u}^2 from the measured E and compare our results with these earlier investigations. This is not justified in view of variations by a factor of two among the results of these investigators which are collected in reference 5. Furthermore, the energy spectrum is best discussed in terms of the three dimensional spectrum E .

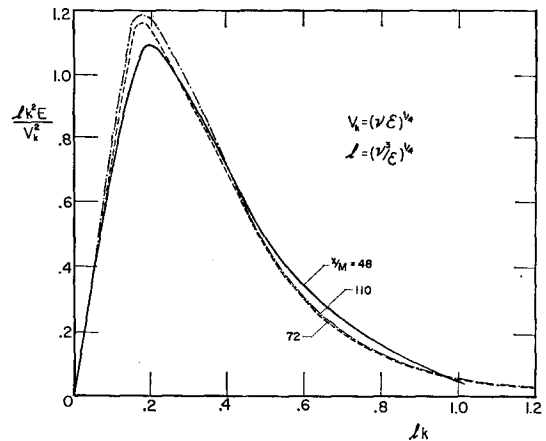


FIG. 20. Universal similarity of small eddies.

⁴ A. N. Kolmogoroff, *Compt. Rend. Acad. Sci. URSS* 31, 538 (1941).

⁵ H. L. Grant, R. W. Stewart, and A. Moillet, *J. Fluid Mech.* 12, 241 (1962).

Before Kolmogoroff presented his theory the kinetic energy $\frac{1}{2}(\overline{u^2} + 2\overline{v^2})$ and the length

$$\lambda = \left[\frac{5\nu(\overline{u^2} + 2\overline{v^2})}{-\frac{1}{2}(d/dt)(\overline{u^2} + 2\overline{v^2})} \right]^{\frac{1}{2}} = \left[\frac{5 \int_0^\infty E dk}{\int_0^\infty Ek^2 dk} \right]^{\frac{1}{2}},$$

were taken as characteristic parameters for small scale motion so that $2\lambda^2 E/(\overline{u^2} + 2\overline{v^2})$ is a function of λk . Figure 21 shows that measurements approximately confirm this similarity. The reason being that for grid turbulence,

$$(\overline{u^2} + 2\overline{v^2}) \sim (t - t_0)^{-n} \sim t^{-n} \quad \text{neglecting small } t_0;$$

therefore

$$\lambda \sim t^{\frac{1}{2}},$$

$$v_k^2 \sim t^{-\frac{1}{2}(n+1)},$$

and

$$l \sim t^{\frac{1}{2}(n+1)}.$$

For $n = 1.2$ the dependence of the two sets of parameters on t is approximately similar and is exactly so for $n = 1$. Some investigators⁶ find from decay of turbulence that $n = 1$; however, they did not report that $\overline{v^2} = \overline{w^2} < \overline{u^2}$ which is always found to be the case.⁷ Since the requirements of Kolmogoroff's theory of local isotropy are satisfied, we expect that the turbulence behind the grid should be, but is not strictly locally isotropic. Assuming local isotropy

$$\left(\frac{\partial v}{\partial x} \right)^2 / \left(\frac{\partial u}{\partial x} \right)^2 = 2$$

and the measurements show that this ratio is at

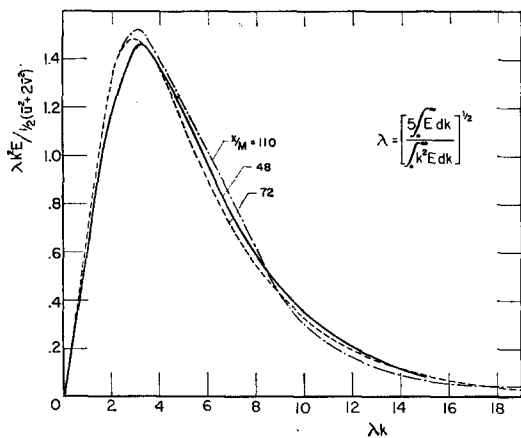


FIG. 21. Similarity of small scale eddies with λ and $(\overline{u^2} + 2\overline{v^2})$ as parameter.

⁶ G. K. Batchelor and A. A. Townsend, Proc. Roy. Soc. (London) **A193**, 539 (1948).

⁷ S. Corrsin, California Institute of Technology, thesis (1942). M. S. Uberoi, J. Aero. Sci. **23**, 754 (1956).

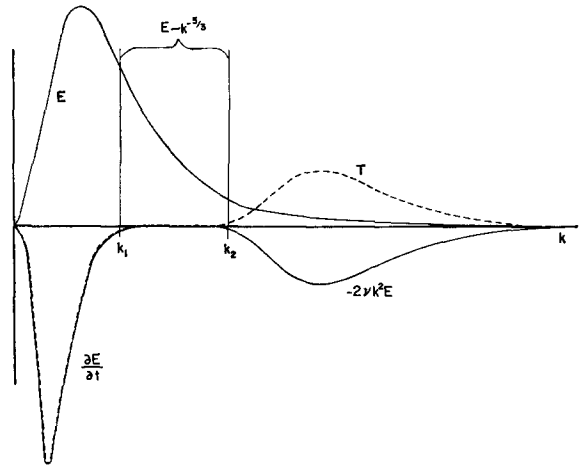


FIG. 22. General nature of the function when inertial subrange exists.

least 40% below the above value. Kistler⁸ finds the same results for much higher grid Reynolds numbers. It appears that Kolmogoroff's theory gives the right parameters for similarity even though the above relation for local isotropy is not satisfied by 40%. We have further investigated the anisotropy of grid turbulence and the possibility of making it isotropic. These results will be reported elsewhere.

An examination of energy transfer in Fig. 10 shows that Kolmogoroff's second similarity hypothesis ($E \sim k^{-5/3}$) is of course not satisfied in the present case and it is doubtful that appreciable inertial subrange exists for grid turbulence at ten times the Reynolds number of the present experiments.

In the inertial subrange both the rate of change of spectrum $\partial E/\partial t$ and the rate of viscous decay $-2\nu k^2 E$ should be negligible and the general nature of the various functions under these circumstances is shown in Fig. 22.

DECAY OF VORTICITY

From the Eq. (2), we have

$$\int_0^\infty k^2 \frac{\partial E}{\partial t} dk = \int_0^\infty k^2 T dk - 2\nu \int_0^\infty k^4 E dk \quad (25)$$

which is the equation for mean square vorticity $\overline{\omega^2}$, since

$$\overline{\omega^2} = 2 \int_0^\infty k^2 E dk. \quad (26)$$

Thus

$$\frac{d\overline{\omega^2}}{dt} = 2 \int_0^\infty k^2 T dk - 4\nu \int_0^\infty k^4 E dk \quad (27)$$

Rate of production of vorticity Rate of viscous dissipation of vorticity

⁸ A. Kistler (private communication).

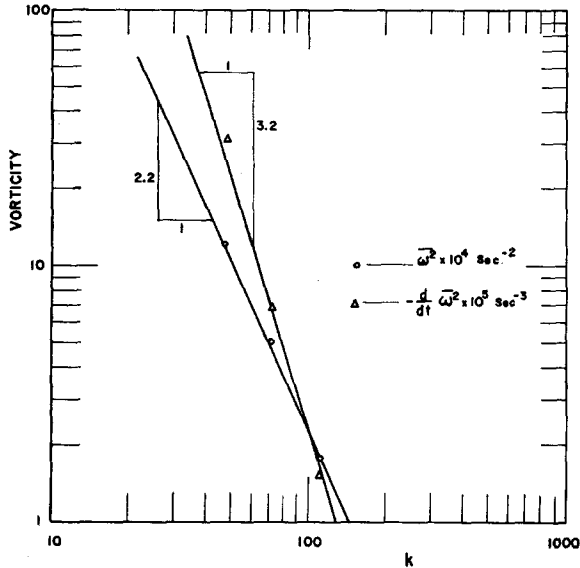


FIG. 23. Vorticity and its decay behind grids.

Kármán and Howarth³ show that

$$\overline{\omega^2} = 15 \left(\frac{\partial u}{\partial x} \right)^2 \tag{28}$$

and

$$\frac{d}{dt} \overline{\omega^2} = -35 \overline{\left(\frac{\partial u}{\partial x} \right)^3} - 70\nu \overline{\left(\frac{\partial^2 u}{\partial x^2} \right)^2}, \tag{29}$$

or

$$\frac{(15)^{\frac{1}{2}}}{35} \frac{d\overline{\omega^2}}{dt} / (\overline{\omega^2})^{\frac{3}{2}} = \frac{\overline{\left(\frac{\partial u}{\partial x} \right)^3}}{\left[\overline{\left(\frac{\partial u}{\partial x} \right)^2} \right]^{\frac{3}{2}}} - 2\nu \frac{\overline{\left(\frac{\partial^2 u}{\partial x^2} \right)^2}}{\left[\overline{\left(\frac{\partial u}{\partial x} \right)^2} \right]^{\frac{3}{2}}} \tag{30}$$

which is another form of the Eq. (27). Since Kolmogoroff's first similarity principle applies here in the Eq. (30) the term on the left is negligible compared with the other two terms which are universal constants approximately equal and of opposite sign. These quantities can be determined from E and T and the results are shown in Figs. 23 and 24. The minor differences between the present results and

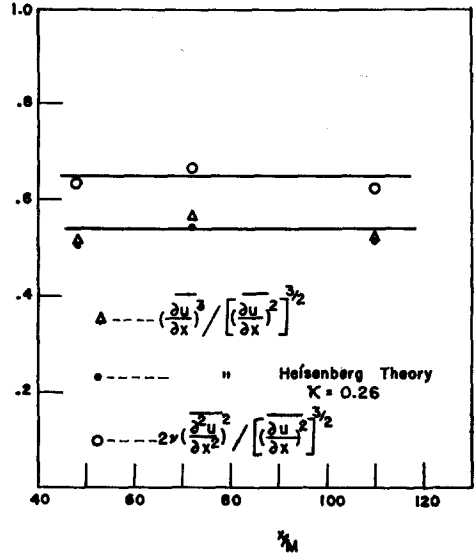


FIG. 24. The quantities

$$-\frac{\overline{\left(\frac{\partial u}{\partial x} \right)^3}}{\left[\overline{\left(\frac{\partial u}{\partial x} \right)^2} \right]^{\frac{3}{2}}} \text{ and } 2\nu \frac{\overline{\left(\frac{\partial^2 u}{\partial x^2} \right)^2}}{\left[\overline{\left(\frac{\partial u}{\partial x} \right)^2} \right]^{\frac{3}{2}}}$$

those given in reference 9 may be due to the slight anisotropy of the grid generated turbulence. We have measured those quantities for $u + \sqrt{2}v$ and have used the condition of the isotropy of turbulence to express them in terms of u . Further, the small eddies are in approximate (within 20%, see Figs. 14 and 15) statistical equilibrium and these constants are not strictly universal but will vary a little with grid Reynolds number. The quantity

$$\frac{\overline{\left(\frac{\partial u}{\partial x} \right)^3}}{\left[\overline{\left(\frac{\partial u}{\partial x} \right)^2} \right]^{\frac{3}{2}}}$$

was also computed from Heisenberg's expression for energy transfer and is shown in Fig. 24.

ACKNOWLEDGMENTS

This work was supported by the Fluid Dynamics Division of the Office of Naval Research under Contract Nonr 1224(02).

The assistance of Stanley Wallis is gratefully acknowledged.

⁹ G. K. Batchelor and A. A. Townsend, Proc. Roy. Soc. (London) **A190**, 534 (1947); *ibid.* **199**, 238 (1949).